



**HAL**  
open science

## Design and multi-physical properties of a new hybrid hemp-flax composite material

J. Page, M. Sonebi, Sofiane Amziane

► **To cite this version:**

J. Page, M. Sonebi, Sofiane Amziane. Design and multi-physical properties of a new hybrid hemp-flax composite material. *Construction and Building Materials*, 2017, 139, pp.502 - 512. 10.1016/j.conbuildmat.2016.12.037 . hal-01652368

**HAL Id: hal-01652368**

**<https://hal.science/hal-01652368>**

Submitted on 28 Feb 2019

**HAL** is a multi-disciplinary open access archive for the deposit and dissemination of scientific research documents, whether they are published or not. The documents may come from teaching and research institutions in France or abroad, or from public or private research centers.

L'archive ouverte pluridisciplinaire **HAL**, est destinée au dépôt et à la diffusion de documents scientifiques de niveau recherche, publiés ou non, émanant des établissements d'enseignement et de recherche français ou étrangers, des laboratoires publics ou privés.



Distributed under a Creative Commons Attribution - NonCommercial 4.0 International License



**QUEEN'S  
UNIVERSITY  
BELFAST**

## **Design and multi-physical properties of a new hybrid hemp-flax composite material**

Page, J., Sonebi, M., & Amziane, S. (2017). Design and multi-physical properties of a new hybrid hemp-flax composite material. *Construction and Building Materials*, 139, 502-512. [1].  
<https://doi.org/10.1016/j.conbuildmat.2016.12.037>

### **Published in:**

Construction and Building Materials

### **Document Version:**

Peer reviewed version

### **Queen's University Belfast - Research Portal:**

[Link to publication record in Queen's University Belfast Research Portal](#)

### **Publisher rights**

© 2016 Elsevier Ltd. This manuscript version is made available under the CC-BY-NC-ND 4.0 license <http://creativecommons.org/licenses/by-nc-nd/4.0/> which permits distribution and reproduction for non-commercial purposes, provided the author and source are cited.

### **General rights**

Copyright for the publications made accessible via the Queen's University Belfast Research Portal is retained by the author(s) and / or other copyright owners and it is a condition of accessing these publications that users recognise and abide by the legal requirements associated with these rights.

### **Take down policy**

The Research Portal is Queen's institutional repository that provides access to Queen's research output. Every effort has been made to ensure that content in the Research Portal does not infringe any person's rights, or applicable UK laws. If you discover content in the Research Portal that you believe breaches copyright or violates any law, please contact [openaccess@qub.ac.uk](mailto:openaccess@qub.ac.uk).

# 1 Design and multi-physical properties of a new 2 hybrid hemp-flax composite material

---

3 J. Page<sup>a,\*</sup>, M. Sonebi<sup>b</sup>, S. Amziane<sup>c</sup>

4 <sup>a</sup> ESITC Caen, 1 rue Pierre et Marie Curie, 14610 Epron, France

5 <sup>b</sup> School of Natural and Built Environment, Queen's University Belfast, University Road, Belfast BT7 1NN,  
6 Northern Ireland, UK

7 <sup>c</sup> Institut Pascal, Clermont Université UMR 6602, 2 avenue Blaise Pascal, 63178 Aubière, France

8 \* Corresponding author. E-mail address: jonathan.page@esitc-caen.fr (J. Page).

## 9 ARTICLE INFO

---

10 *Keywords :*

11 Hemp concrete

12 Flax fibers

13 Water absorption

14 Mechanical properties

15 Shrinkage

16

## 17 HIGHLIGHTS

---

- 18 • The incorporation of the flax fibers has increased the ductility of the hemp concrete.
- 19 • Flax fibers have improved the compressive strength of hemp concrete.
- 20 • The hybrid composite appears to have a lower water absorption than hemp concrete.
- 21 • Hemp-flax hybrid concretes showed a lower shrinkage of about 15% compared to conventional  
22 hemp concrete.

23

24

## 25 ABSTRACT

---

26 An experimental investigation was conducted in order to study the properties of a hybrid hemp-  
27 flax composite material in term of capillary water absorption, mechanical strength, thermal  
28 conductivity and shrinkage. The hemp-flax composite material is made with 90% hemp shives and  
29 10% flax fibers. Hemp aggregates have a high water absorption capacity, which led to a reduction of  
30 the hemp concrete mechanical performances. Four mixes were made for: shuttered walls, external  
31 coating, floor insulation and roof insulation. Firstly, bio-based aggregates were characterized in term  
32 of particle size distribution and water absorption. Then, the compressive strength of these four mixes  
33 was determined to compare the mechanical behavior of the hybrid composite material with hemp  
34 concrete. The capillary absorption and the total shrinkage of these bio-based materials were also  
35 measured. Finally, we measured the thermal conductivity coefficient of these materials. The results  
36 of the compressive strength show a significant improvement due to the incorporation of flax fibers.  
37 Flax fibers improve the compactness of the material, thus increasing its density, which leads to a  
38 greater mechanical strength. It was observed that the capillary absorption of hemp concrete seems to  
39 be related to the aggregates/paste ratio. Finally, flax fibers have reduced hempcrete shrinkage of  
40 about 15%.

## 41 **1. Introduction**

42 Currently, the construction industry is responsible for 24% of carbon dioxide emissions and 44%  
43 of the energy consumption in France [1]. New building insulation standards tend to decrease the  
44 amount of energy used for heating, which accounts for almost two thirds of the energy consumption  
45 and the main part of the CO<sub>2</sub> emissions in the building sector in France. However, in this context, energy  
46 expenditure devoted to the manufacture and the implementation of construction materials is  
47 increasing. Regarding France's commitments to the Kyoto protocol for 2050, the development of new  
48 materials based on renewable resources is necessary.

49 Plants have been largely forgotten by modern technologies. The evolution of production processes,  
50 the need for materials compatible with sustainable construction, consumer expectations and  
51 regulatory requirements mean that bio-based materials are becoming increasingly interesting. Among  
52 the plants usable for construction, hemp certainly has a privileged position and can be considered as a  
53 model. Hemp stands out because of its environmental assets such as its contribution to the  
54 improvement of the soil, its neutral carbon accounting, its low embodied energy expenditure and its  
55 end of life without harmful consequences for the environment [2]. From hemp is extracted shiv, which  
56 is mostly used as litter for animals thanks to its absorbent properties [3]. However, hemp shiv can be  
57 mixed with binders (lime and/or cement) and water to make hemp concrete.

58 Hemp-lime concrete is used only for twenty years in construction in France. It is most frequently  
59 used in lining or filling to form a construction element having good thermal and sound insulation  
60 without structural contribution. For ten years, many researches have been conducted on this material,  
61 which now allows a better understanding of its properties [4]. Most published researches are focused  
62 on its acoustical, thermal and hygrothermal properties which result from the highly porous structure  
63 of hemp shiv [5-8]. Hemp concrete is a lightweight composite insulating material having a dry density  
64 ranging from 200 to 800 kg.m<sup>-3</sup> [9]. This low density gives to hempcrete its high thermal properties.  
65 Indeed, its dry thermal conductivity is between 0.06 and 0.12 W.m<sup>-1</sup>.K<sup>-1</sup>, depending on mix  
66 formulations. However, this porous structure also resulted in low strength and low rigidity of the  
67 material after curing. Generally, in most studies, hemp concrete compressive strength remained  
68 relatively low compared to other conventional building materials, often less than 1 MPa [10-14].

69 However, a comparative study realized in 10 different laboratories, on identical hemp concrete  
70 formulations, showed that this material has an accurate repeatability regarding the density and the  
71 mechanical strength [15].

72 Given this low mechanical strength, hemp concrete cannot therefore be used as a load bearing material.  
73 This material is also characterized by an important mechanical ductility, with a compressive strain  
74 higher than 10 % [10]. The literature suggests that the high absorption capacity of lignocellulosic  
75 aggregates, sometimes greater than 300 % by mass, is one of the main causes of hemp concrete low  
76 mechanical performances [16]. It induces a decrease of the water available for the binder setting,  
77 which leads to poor binder-aggregate interface.

78 Hemp concrete is often directly implemented on the construction site, or manually into forms or by  
79 projection process [12]. These methods of implementation do not allow reaching a sufficiently high  
80 compactness. However, previous work has shown that the compaction of hemp concrete at fresh state  
81 led to an increase of the mechanical performances [17,18]. Hemp aggregates have a particle size  
82 distribution predominantly between 1 and 5 mm [19]. Flax fibers have diameters around 5 to 80  
83 microns [20]. Flax fibers can therefore be inserted between hemp aggregates and thus increase the  
84 compactness of the composite. In addition, the flax fibers can help to improve the behavior of the hemp  
85 concrete in large strains and thereby increase its ductility [21].

86 This experimental work aims to study the effect of incorporating flax fibers on the performances of  
87 lime-hemp composite. For this purpose, the physical, mechanical and thermal properties of the hybrid  
88 hemp-flax composite were studied and compared to conventional hemp concrete. First of all, the water  
89 absorption flax fibers and hemp shives was measured. Then, the particle size distribution of hemp shiv  
90 was determined by image analysis. Four formulations were made to study the properties of these bio-  
91 based composites. These formulations were based on the French professional execution rules for hemp  
92 concrete, published in 2012 [22]. These standard practices provide four hemp-lime concrete mix  
93 designs for four different applications: external coating, shuttered wall, floor insulation and roof  
94 insulation. Thus, through these four formulations, hybrid hemp- flax composite properties were  
95 measured and compared to conventional hemp concretes.

96 **2. Materials and methods**

97 *2.1. Raw materials*

98 *2.1.1. Hemp aggregates and flax fibers*

99 Hemp shiv used as aggregates for this study was Tradical® HF. It is a hemp aggregate made from  
100 the inner woody core of the hemp plant's stem. Hemp is chopped, graded and de-dusted to give a  
101 natural, sound and breathable product. This type of shiv is compatible with lime-based binders and is  
102 marketed for individual housing construction in hemp concrete. Its absolute density, obtained with a  
103 gaz pycnometer, is equal to 1.48. Hemp shiv is characterized by its low bulk density [23], about 110  
104 kg.m<sup>-3</sup>, which additionally gives it a very low thermal conductivity of approximately 0.048 W.m<sup>-1</sup>.K<sup>-1</sup>,  
105 determined with the transient hot-wire method [24].

106 Elementary flax fibers used for this work have a length of 12.7 mm, with a diameter ranged between  
107 43 and 53 microns and were grown in Italy. For this work, only untreated fibers were used.  
108 Monofilament flax fibers are used to improve cohesion, holding, mold-ability, and to limit the cracking  
109 of cementitious composites.

110 *2.1.2. Mineral binder*

111 The binder used in this study was Tradical® PF70. It has already used in several other researches  
112 for making hemp concrete [2,6,18,25]. It is a special lime binder based on aerial lime (75%), hydraulic  
113 binder (15%) and pozzolanic binder (10%).

114 This binder has been chosen for its great capacity to generate carbonation reactions. Indeed, aerial  
115 lime contains a large amount of calcium hydroxide Ca(OH)<sub>2</sub> [16]. Once mixed with water and  
116 aggregates and in the presence of carbon dioxide, carbonation of the lime takes place, converting  
117 calcium hydroxide into calcium carbonate (CaCO<sub>3</sub>). This is a very slow reaction. It starts mainly when  
118 lime has sufficiently dried and can last for months or even years. Then, the hydraulic binder (15 % of  
119 the composition) allows a higher reactivity and better short term resistance. Indeed, dicalcium and  
120 tricalcium silicates present in the binder will react with water to form calcium silicate hydrates (C-S-

121 H) and portlandite. Finally, the pozzolanic binder (10% of the composition) will react with calcium  
122 hydroxide  $\text{Ca}(\text{OH})_2$  during the cement hydration and will promote the formation of calcium silicate  
123 hydrates [16].

## 124 2.2. Methodology

### 125 2.2.1. Mix design

126 According to the French professional execution rules for hemp concrete structures [22], four  
127 different mixtures were used throughout this work:

- 128 • Mix C: external Coating.
- 129 • Mix W: shuttered Walls.
- 130 • Mix F: Floor insulation.
- 131 • Mix R: Roof insulation.

132 Amziane and Arnaud provide dosages based on experience for these four applications [9]. Mix  
133 proportions by mass and notations used are presented in Table 1.

134 Two different concrete families have been formulated for this study. The first is a conventional  
135 hemp concrete, wherein all the introduced aggregates are hemp shives. This concrete will be noted  
136 later HC for Hemp Concrete. In the second hemp concrete, 90 % (in mass) of the aggregates are hemp  
137 shives and the remaining 10 % are flax fibers. Hemp shives are therefore substituted partially (10% in  
138 mass) by flax fibers. This second composite will be abbreviated FHC for Flax-Hemp Concrete.

139 **Table 1.** Composition in dry mass of each mixes for a batch of 1000 g.

		Aggregates		Binder	Water	A/W	A/B
		Hemp shiv	Flax fibers			mass ratio	mass ratio
<b>Mix C</b>	HC	170 g	-	360 g	470 g	0.36	0.47
	FHC	153 g	17 g				
<b>Mix W</b>	HC	230 g	-	310 g	460 g	0.50	0.74
	FHC	207 g	23 g				
<b>Mix F</b>	HC	220 g	-	410 g	370 g	0.59	0.54



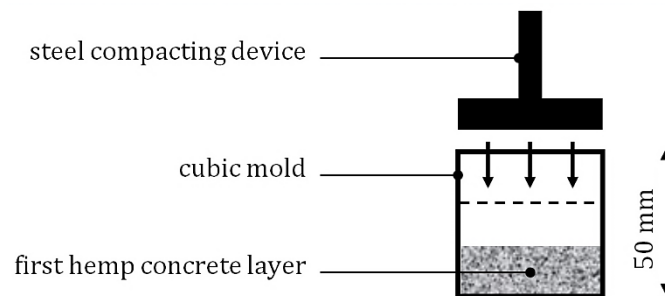
	FHC	198 g	22 g				
<b>Mix R</b>	HC	320 g	-	220 g	460 g	0.70	1.45
	FHC	288 g	32 g				

140 *2.2.2. Mixing procedure*

141 One of the main difficulties encountered during the hemp concrete mixing is due to the water  
 142 absorption of plant aggregates. This water absorption creates a problem for the binder which needs to  
 143 be hydrated [18]. For this reason, it is essential to take into account the water absorption capacity of  
 144 the raw natural particles. Thus, hemp shives and flax fibers were first pre-wetted in the mixing drum  
 145 during 2 minutes with 65% of the water quantity. Then, the binder was added and mixed during 1  
 146 minute. Finally the remaining water (35%) was introduced in the mixing drum and mixed during 2  
 147 minutes. The total mixing time was equal to 5 minutes.

148 *2.2.3. Casting procedure and curing conditions*

149 The concrete was poured in the different molds: 50 x 50 x 50 mm<sup>2</sup> cubs for compressive test and  
 150 100 x 100 x 100 mm<sup>2</sup> cubs for capillary water absorption measurement. They were compacted in three  
 151 layers by using a steel manual device (Fig. 1). The height of a single layer is equal to one-third of the  
 152 total height of the concrete specimen (50 or 100 mm). The first and second layers have been scratched  
 153 to obtain a good grip surface for the next layer. Specimens were demolded after 24 h and stored in a  
 154 climate-controlled room at 20 °C and 60 %RH.



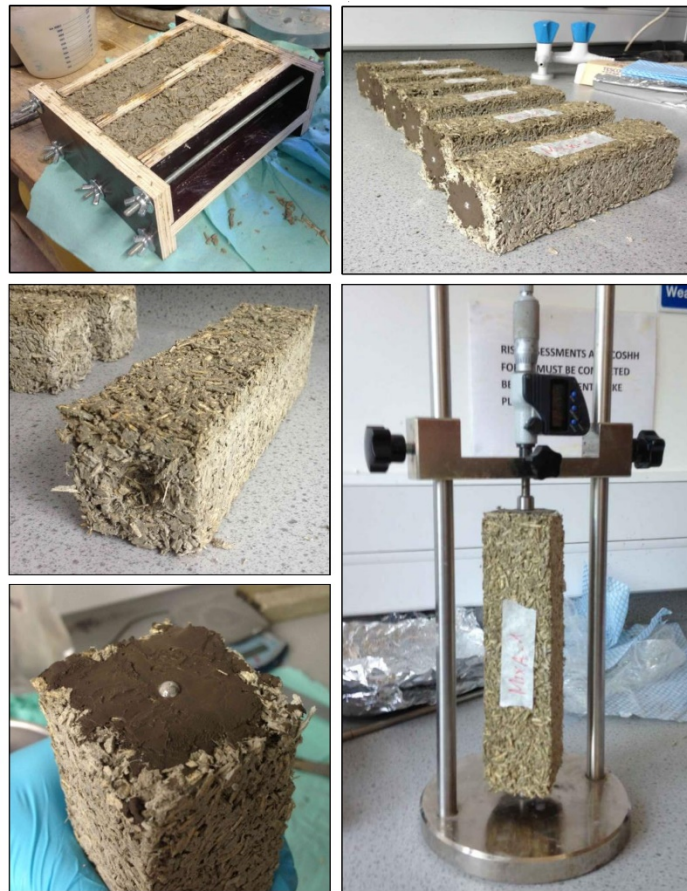
155

156

**Fig. 1.** Compaction process.

157 The shrinkage was measured on prism of 50 x 50 x 200 mm. A shrinkage measurement device has  
 158 been used, so it was necessary to place a metallic ball on both ends of each specimen. To place these  
 159 balls, a hole was dug at each end of the specimens after release. Then, a quick-setting mortar has been

160 made and applied in holes. Finally, ball was placed in the hole and was semi-embedded in mortar (Fig.  
161 2). The fixation of the ball is a crucial step for the shrinkage measurement.



162

163

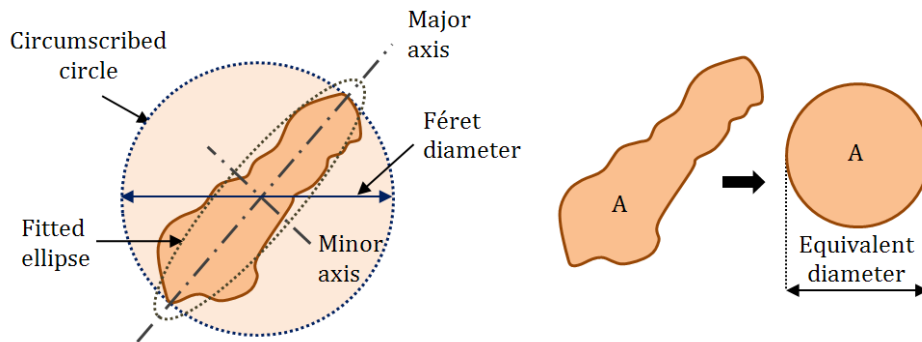
**Fig. 2.** Prisms manufacturing and shrinkage measurement.

### 164 *2.3. Experimental procedures*

#### 165 *2.3.1. Hemp shiv particle size distribution by image analysis*

166 Previous studies have shown that image analysis is the most efficient method to characterize the  
167 particle size distribution of hemp shiv [16,17]. Indeed, because of the elongated shape of hemp  
168 particles, the particle size distribution by mechanical sieving is inappropriate [26]. In order to compare  
169 the results with image analysis, a particle size by sieving of hemp shiv has nonetheless been achieved  
170 according to EN 933-2 [27]. This method of characterization is recommended by the RILEM Technical  
171 Committee 236-BBM [23].

172 The image analysis has been done with ImageJ software. This software uses a method called "best  
173 fitting ellipse" to calculate morphological parameters, such as the major and minor axes (



174

175 **Fig. 3).**

176 The main advantage of this method compared to sieve grading is to obtain a characterization of  
177 complex particle morphology and heterogeneity. Nevertheless, this technique is limited to small  
178 aggregate quantities (some grams) and hemp hurd residual fibers cannot be detected. Three different  
179 random samples of at least 2000 particles were placed on a black sheet of paper. Then the digital  
180 acquisition is treated with the image processing software. The morphological parameters selected for  
181 analysis are the following:

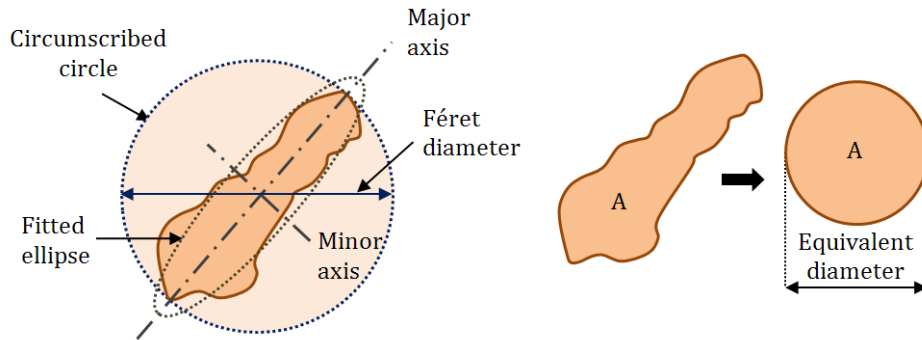
- 182 • Major axis dimension (major): length of the longest axis of the fitted ellipse.
- 183 • Minor axis dimension (minor): length of the shortest axis of the fitted ellipse (perpendicular to  
184 the major axis).
- 185 • Particle area (A): area of the aggregate, measured by the number of pixels.
- 186 • Particle perimeter (P): contour of the particle in pixels.
- 187 • Equivalent diameter (ED): the diameter of a circle having the same area as the object, defined as:

$$ED = \sqrt{\frac{4 * A}{\pi}} \quad (1)$$

- 188 • Elongation: ratio between the major axis and the minor axis. Its value is all the time greater  
189 than 1.

- 190 • Circularity: its value ranges from 0 (infinitely elongated particle) to 1 (perfect sphere),  
 191 calculated as follows:

$$\text{Circularity} = 4\pi * \frac{A}{P} \quad (2)$$



192

193

**Fig. 3.** Definition of calculated geometric parameters.

194 *2.3.2. Plant particles water absorption*

195 Due to their porous structure, hemp shiv and flax fibers are very sensitive to water [10,28]. The  
 196 protocol used to measure water absorption is as follows [29,30]:

- 197 1. Dry 200 grams of aggregates at 60°C up to ± 0.1% mass variation in 24 hours is achieved.
- 198 2. Put a synthetic or metallic bag (with holes around 1 mm<sup>2</sup>) in water for a complete wetting.
- 199 3. Put the bag in a salad spinner and turn it 100 times at approximately 2 rotations per second.
- 200 4. Tare the spinned bag and note the value.
- 201 5. Weight 25 grams (M<sub>0</sub>) of dry aggregate and put it in the water permeable bag.
- 202 6. Put the bag of aggregates in water for 1 minute.
- 203 7. Put this bag in a salad spinner and turn it 100 times at approximately 2 rotations per second.
- 204 8. Weight the spinned aggregates bag and note the M<sub>1</sub> value (1 min).
- 205 9. Repeat steps 6, 7 and 8 with another the sample at different times: 15, 240 and 2880 minutes.

206 10. Calculate the value of absorption with this formula:

$$M(t) = \frac{M_t - M_0}{M_0} * 100 \quad (3)$$

207 The water absorption has been measured on hemp shiv and on flax fibers. In order to see the  
208 repeatability, this test was carried out three times for each aggregate. This method of characterization  
209 is recommended by the RILEM Technical Committee 236-BBM [31].

### 210 2.3.3. *Compressive tests*

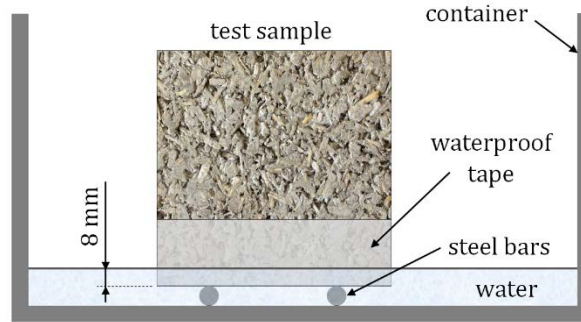
211 Compression tests were performed after 7 and 28 days of curing in a climate-controlled room (20  
212 °C and 60 %RH) by using an electromechanical testing machine with a 50 kN capacity. They were  
213 conducted on 50 x 50 x 50 mm cubes with a 3 mm.min<sup>-1</sup> speed. Three replications were done for each  
214 mix.

### 215 2.3.4. *Capillary water absorption*

216 Capillary water absorption was measured after 7 days of curing in a climate-controlled room (20 °C  
217 and 60 %RH) by using a cube of 100 mm size. Then, the specimens were dried during 24h before  
218 testing. Two replications were done for each mix.

219 The purpose of this test is to simulate a capillary rising in a masonry wall, in order to assess the  
220 concrete behavior towards water. A waterproof tape was applied around the circumference of the test  
221 piece. Test pieces were then placed in a plastic container on two steel bars (to ensure water absorption  
222 only on the underside of the specimen). Finally, the container was filled with water until obtain an  
223 imbibition front of 8 mm. Water level was maintained to 8 mm during the time of the experiment (Fig.  
224 4).

225 The specimens initial dry mass is first measured ( $M_0$ ). Then, the specimens were weighed after  
226 different time of immersion in water ( $M_t$ ). The Eq. 3 has been used to calculate the capillary water  
227 absorption.



228

229

**Fig. 4.** Measuring system of capillary water absorption.

230 *2.3.5. Shrinkage measurement*

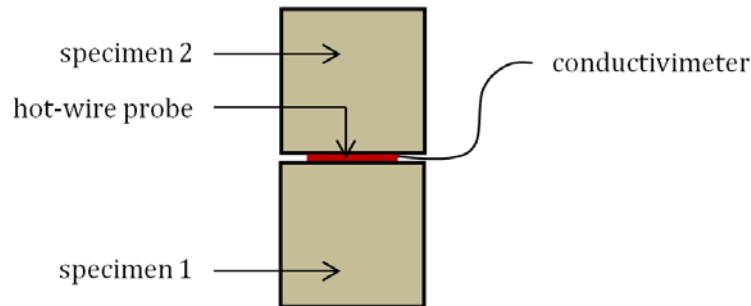
231 Two samples of each mix were tested using French cement standard NF P15-433 [32]. The  
 232 specimens were stored in a climate-controlled room (20 °C and 60 %RH) during all the measurement  
 233 of the total shrinkage. Measurements were made using a shrinkage apparatus having an accuracy of  
 234 0.001 mm and performed every 2-4 days up to 46 days (Fig. 2).

235 *2.3.6. Thermal conductivity*

236 Thermal conductivity of HC and FHC specimens was measured with a thermal apparatus  
 237 (conductivimeter) using the transient hot-wire method, according to EN ISO 8894 [33]. This method  
 238 consists in generating a heat flow by Joule effect and measuring the temperature variation over time  
 239 by means of a thermocouple. This thermocouple is associated with the heating element in the hot-wire  
 240 probe. The rise in temperature measured by the sensor is limited to 20°C and the measuring time is  
 241 dependent on the material, here taken as 60 seconds. The temperature variation ( $\Delta T$ ) is related to the  
 242 electrical power (P), the wire length (L) and the thermal conductivity ( $\lambda$ ) [34]. If the temperature is  
 243 measured at times  $t_1$  and  $t_2$ , the thermal conductivity is given by the following equation:

$$\lambda = \frac{P}{4 \cdot \pi \cdot L \cdot \Delta T} * \ln\left(\frac{t_2}{t_1}\right) \quad (4)$$

244 Measurements were done by positioning the thermal probe between two specimens of same mix  
245 (Fig. 5) and have been tested three times. This method of characterization is recommended by the  
246 RILEM Technical Committee 236-BBM [24].



247

248 **Fig. 5.** Thermal conductivity measurement by the transient hot-wire method.

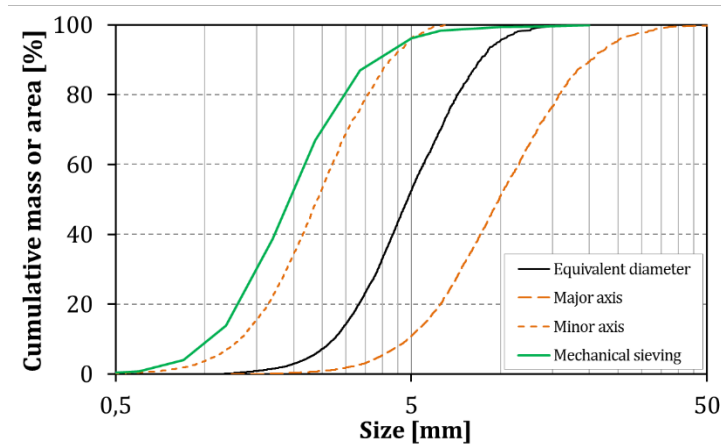
### 249 **3. Results and discussion**

#### 250 *3.1. Plant particles characterization*

##### 251 *3.1.1. Particle size distribution*

252 The particle size by sieving is the reference standard for characterizing mineral aggregates [27].  
253 For lignocellulosic shives, the square mesh sieves are inadequate because they do not take into account  
254 the elongation of aggregates [26]. In Fig. 6, the particle size distribution of the shives produced by  
255 mechanical sieving is between 0.5 and 5 mm. The particle length seems unlikely to change. Only the  
256 thickness and width of the particle condition the passage from one sieve to another.

257 Image analysis provides considerably more exhaustive information than the mechanical sieving.  
258 Fig. 6 reveals, in contrast to sieving, significant differences between the major and minor axes and the  
259 equivalent diameter. The median equivalent diameter is equal to 4.86 mm and the gap between the  
260 median  $D(a, 0.5)$  of the minor and major axes equal to 7.49 mm. At first sight, this reflects a great  
261 heterogeneity of the hemp aggregate. However, these values are consistent with the literature.  
262 Chabannes, for example, has found for its hemp shiv, an equivalent diameter of about 5 mm and a gap  
263 between the median of the minor and major axis approximately equal to 6.8 mm [35]. Nozahic, for its  
264 part, find for these two parameters, values equal respectively to 4.2 mm and 6.2 mm [36].



265

266

**Fig. 6.** Hemp shiv particle size curves obtained by image analysis and mechanical sieving.

267

The parameters derived from the image analysis are used to express other morphological criteria such as elongation and circularity (Fig. 7).

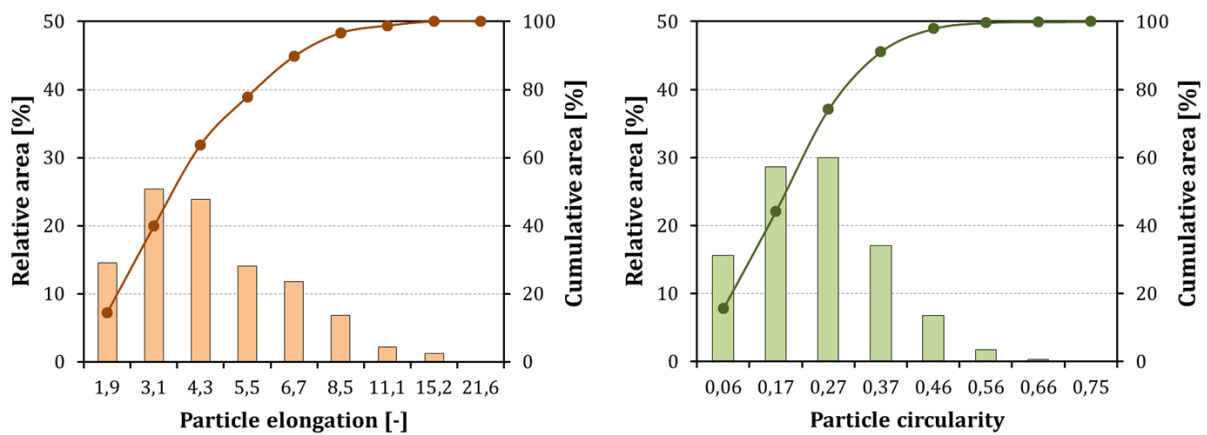
269

The elongation corresponds here to the calculated ratio between the dimension of the two axes of the ellipse (major axis / minor axis). The elongation follows a lognormal distribution. One hemp shiv population is present and which may have an elongation of up to 8 or more. The median value of the elongation ratio is  $3.82 \pm 2.33$ . Generally, elongation is very high, which does not favor the granular particle arrangement.

274

The circularity of the particles is also log-normally distributed. The median value of the circularity ratio is very low, about  $0.26 \pm 0.14$ . This confirms the high elongation of hemp aggregates.

275



276

277

**Fig. 7.** Hemp shiv particle elongation and circularity.



278 3.1.2. Water absorption

279 The absorption kinetics, measured by sequential weighing after immersion in water, is similar for  
280 both aggregates (Fig. 8). The water absorption is very fast to these two particles. These dry aggregates  
281 absorb more than a third of their maximum absorption capacity in less than a minute. The measured  
282 water absorption values are consistent with the literature [14,16,28]. The water absorption measured  
283 after 48 hours of immersion is about 450 % for hemp and over 200 % for flax fibers. The difference in  
284 the amount of water absorbed between hemp shiv and flax fibers can be explained by a lower  
285 hydrophilicity of the fibers, due to a less porous structure compared to hemp shives [9].

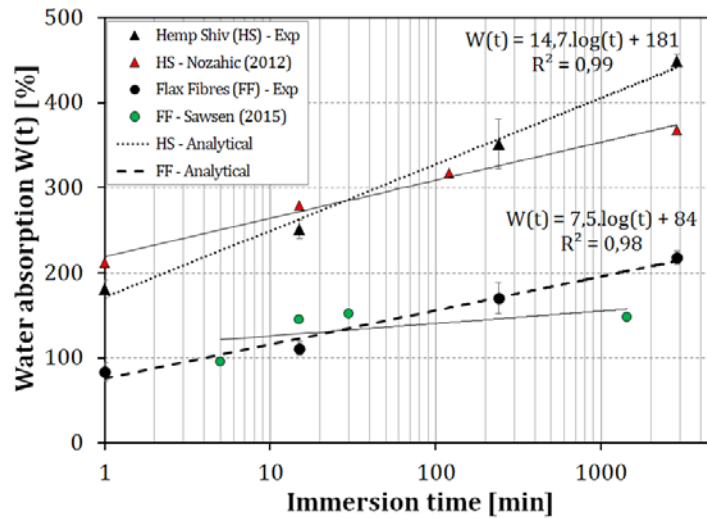
286 Two phases of absorption can be observed. The first one is a surface absorption phase which causes  
287 an almost instantaneous increase of the aggregate mass. It highlights the rapid nature of the wetting  
288 of hemp and flax particles. The second phase is the slow absorption into the vegetable structure. This  
289 demonstrates the diffusive behavior of the water propagation in the structure up to 48 hours. The  
290 wetting phase may be considered completed after 1 minute. The initial absorption  $W_0$  was set for this  
291 duration. On this value, an important difference is visible between hemp ( $W_0 = 181$  %) and flax ( $W_0 =$   
292 84 %).

293 It is visible in Fig. 8 that the intra-granular water absorption follows a logarithmic law. Nozahic has  
294 defined the following relationship is valid until saturation aggregates [36]:

$$W(t) = C_A * \log(t) + W_0 \quad (4)$$

- 295 •  $W_0$  : Initial water absorbed by the particles (1 min) ;
- 296 •  $C_A$  : Water absorption coefficient of particles.

297 The water absorption capacity of bio-aggregates has a significant role in the formulation and  
298 implementation of hemp concrete. This hydrophilic property of vegetable particles influences the  
299 binder setting [18]. Indeed, hemp shiv and binder will be in competition to mobilize water, thereby  
300 altering the binder hydration.



301

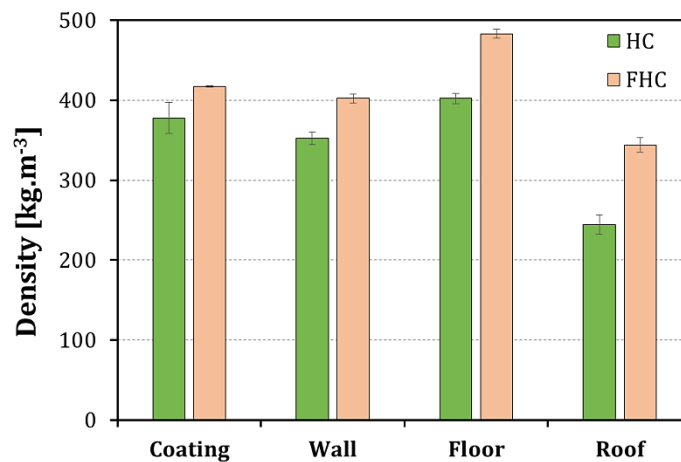
302

**Fig. 8.** Water absorption of hemp shives and flax fibers.

303 *3.2. Physical properties of bio-based concretes*

304 *3.2.1. Bulk density*

305 Fig. 9 presents the bulk densities obtained for HC and FHC after 28 days curing. It ranges from 250  
 306 to 500 kg.m<sup>-3</sup>, depending on mix formulation. The hemp concrete density is lower than ordinary  
 307 concrete. It is this low density, which gives to hemp concrete its good thermal properties. Substituting  
 308 10% of the mass of hemp shives by an identical mass of flax fibers significantly affects the density of  
 309 the material. Indeed, the density increased from 10.3 % to 40.4 % depending on the formulation.

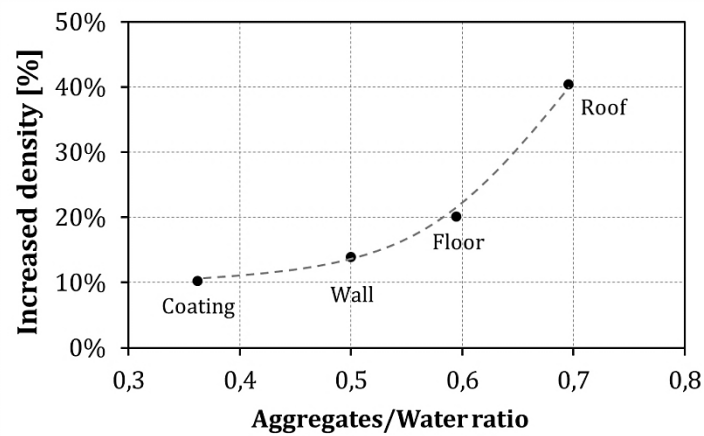


310

311

**Fig. 9.** Densities of HC and FHC after 28 days curing.

312 In Fig. 10, it can be observed the density increased between HC and FHC concretes according to the  
 313 A/W mass ratio. The density of hybrid hemp-flax concretes increased with A/W ratio and the trend  
 314 follows a quadratic polynomial function. The coefficient of determination was very close to 1. In fact,  
 315 the more the amount of hemp shives increases, the higher intergranular space is. Flax fibres, which  
 316 have diameters smaller than hemp shiv, are insertable into these spaces, thereby led to an increase in  
 317 the compactness. Hence a higher density for hybrid cementitious composites is obtained.



318

319 **Fig. 10.** Increased density between HC and FHC depending on the A/W ratio.

### 320 3.2.2. Capillary absorption

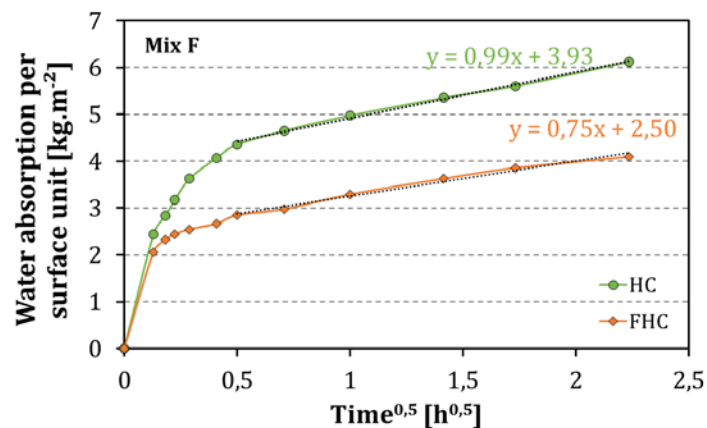
321 Sonebi highlighted that hemp concrete is sensitive to weathering and in particular to wetting-  
 322 drying cycles [37]. He noted a decrease of the mechanical strength from 50 to 80 % after 10 wetting-  
 323 drying cycles, according to the formulations. Therefore the water absorption of hemp concretes is an  
 324 important parameter for the durability of this material.

325 Capillary water absorption can be used as an indicator of the degradation of building materials,  
 326 especially for masonry blocks. It can be described by the water absorption coefficient. The latter results  
 327 from the gradient of the straight line of curves presented in Fig. 11 as the mass of water absorbed  
 328 versus square root of time. This capillary water absorption coefficient is defined as  $C_A$  ( $\text{kg}\cdot\text{m}^{-2}\cdot\text{h}^{-1/2}$ ) by  
 329 the following equation:

$$M_w = C_A * \sqrt{t} + k \quad (5)$$

- 330 •  $k$  is a function of the contact area with water ( $\text{kg}\cdot\text{m}^{-2}$ ) corresponding to the y-intercept of the
- 331 straight line ;
- 332 •  $\sqrt{t}$  is the square root of time.

333 As it can be seen from the results on Fig. 11, the capillary kinetics is similar for the different  
 334 composites. Water absorption is initially increasing, then slows down as time progresses. However,  
 335 there is a significant difference in the rate at which capillary water is absorbed.

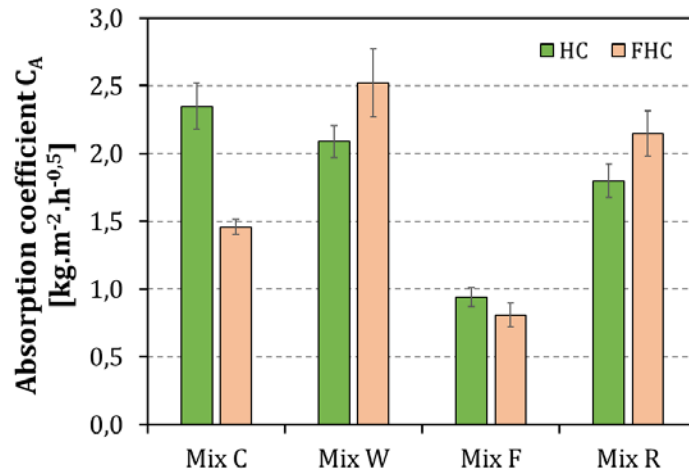


336

337 **Fig. 11.** Capillary water absorption curves for floor insulation mixture specimens (Mix F).

338 The water absorption coefficients are represented in (Fig. 12). They range from 0.81 to 2.52  $\text{kg}\cdot\text{m}^{-2}\cdot\text{h}^{-1/2}$ .  
 339 These values are lower than those observed by Walker [8] (between 2.65 and 3.37  $\text{kg}\cdot\text{m}^{-2}\cdot\text{h}^{-1/2}$ ).  
 340 This can be explained by a measurement of the capillary absorption after only 7 days curing. In  
 341 addition, the imbibition height used by Walker was different (10 mm).

342 The addition of 10% flax fibres seems to decrease capillary absorption of hemp concrete for mixtures  
 343 containing a low proportion of vegetable aggregates. Indeed, the  $C_A$  coefficient is lower for mixes C and  
 344 F. In contrast, the absorption coefficient increased for mixtures containing a higher proportion of  
 345 hemp, i.e. mixtures W and R.



346

347

**Fig. 12.** Absorption coefficients for HC and FHC.

348

Capillary porosity is defined as residual spaces occupied by the original kneading water. Indeed, some studies show that the capillary water absorption of hemp concrete depends on the amount on aggregates [38]. These same results are obtained with the HC (Fig. 13). The more important the aggregates/paste ratio is, the more the maximal capillary water absorption (after 5 hours) increases. In fact, this ratio is known to affect the relative volume of solids and capillary voids. The volume of capillary voids increases with the aggregates amount and the capillary water absorption is strongly linked to capillary voids.

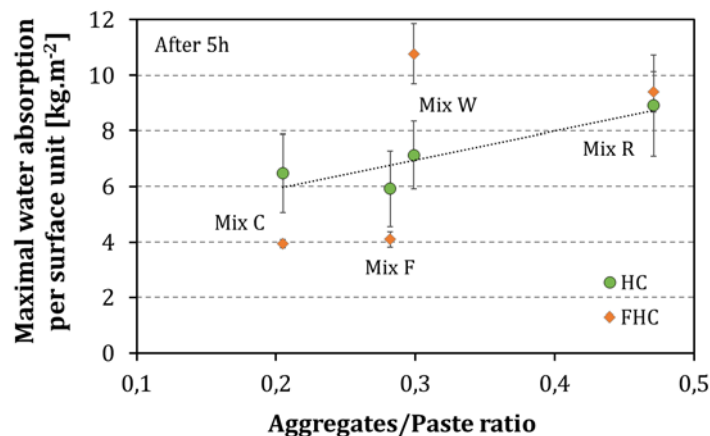
355

However, the relationship between the aggregates/paste ratio and capillary absorption cannot be seen with FHC hybrid concrete. This could be due to an increase of tortuosity of the concrete pore structure due to the presence of flax fibers, which would complicate the capillary suction phenomenon and so the quantity of water absorbed (Fig. 13).

356

357

358

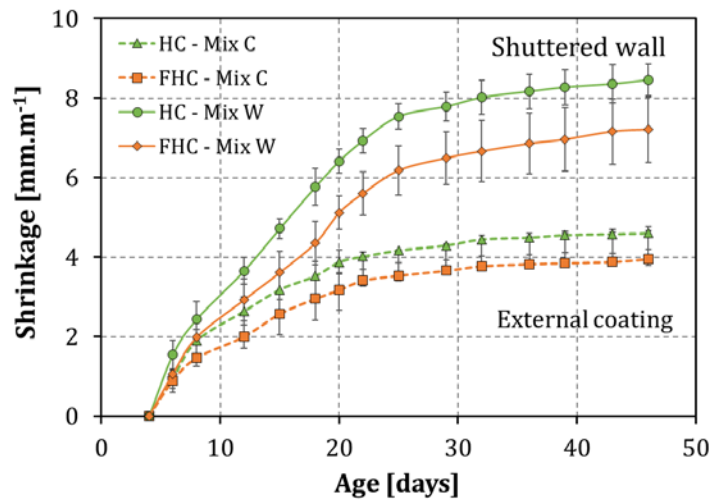


359

360 **Fig. 13.** Maximal water absorption per surface unit according to the aggregates/paste ratio.

### 361 3.2.3. Shrinkage

362 The phenomenon has not been widely investigated for lime and hemp shiv concretes. However,  
363 Murphy and Kashtanjeva studied hemp concrete shrinkage [39,40]. A similar behavior is obtained with  
364 hemp concrete, reinforced with flax fibers or not (Fig. 14). The increase of the shrinkage was relatively  
365 constant up to 25 days. Then the shrinkage continued to increase slowly until the end of the test to 46  
366 days (Fig. 14). The shrinkage stabilised for HC concrete after 25 days, at 8.5 mm.m<sup>-1</sup> for mix W  
367 (shuttered wall) and about 4.5 mm.m<sup>-1</sup> for mix C (external coating). For both mixes, hybrid hemp-flax  
368 concrete has a lower shrinkage of about 15% (7.5 mm.m<sup>-1</sup> for mix W and 4 mm.m<sup>-1</sup> for mix C). As  
369 Murphy, it is possible to see that the wall formulation (mix W) always has a higher shrinkage than the  
370 coating formulation (mix C). Mix W having a higher W/B ratio and a higher amount of hemp, water  
371 mobilization for plant particles will therefore be greater, which may cause a shrinkage increasing.



372

373 **Fig. 14.** Shrinkage measured for HC and FHC.

### 374 3.3. Mechanical properties

#### 375 3.3.1. Influence of compaction direction

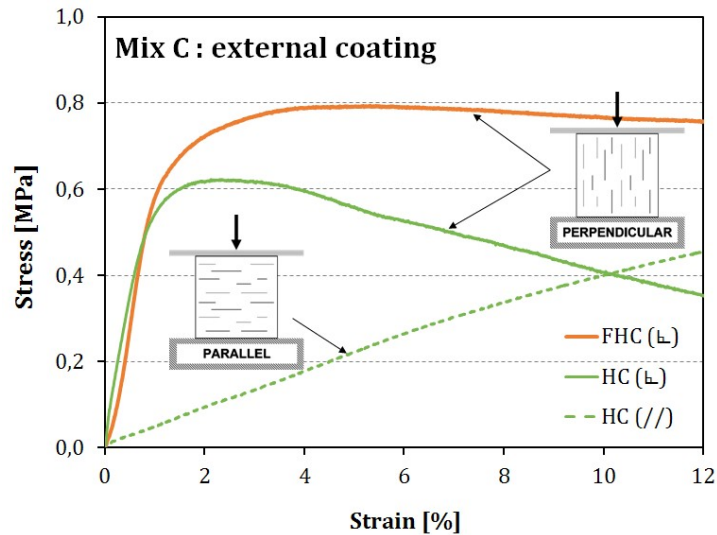
376 Hemp concrete has a different behavior depending on the direction of compaction during the  
377 casting process [16]. Conventionally, hemp concretes are compacted manually and are solicited

378 alongside their compaction direction. The compressive force is thus directed perpendicular to the fiber  
379 orientation due to the implementation. Conversely, when the compression test is performed  
380 perpendicularly to the direction of compaction, hemp shiv particles (oriented compaction) are more  
381 stressed in their longitudinal direction. This is their direction of greater rigidity.

382 Only mix C (external coating) was tested in compression with a direction perpendicular to the  
383 compacting direction. Indeed, mix C is a mixture for an external rendering. For this mixture, hemp  
384 concrete is implemented by projection. For this implementation process, hemp concrete is compacted  
385 perpendicularly to the loading direction. For mixtures W and F (respectively shuttered walls and floor  
386 insulation) the loading direction is parallel to compaction. Finally, for the mix R which corresponds to  
387 roof insulation, the orientation is neither parallel nor perpendicular; it depends on the slope of the  
388 roof.

389 The curve obtained for the mix C with a parallel orientation was also plotted (Fig. 15). It can be  
390 noticed a ductile behavior for this material. There is no brittle fracture; the material has a large  
391 deformation capacity. A compression in the direction orthogonal to the compaction generates a greater  
392 elastic modulus and a higher compressive strength than compression carried out in parallel to  
393 compaction (Fig. 15). In other words, compression performed in parallel to the preferential orientation  
394 plane (longitudinal) of parallelepiped aggregates generates a higher stiffness than when stress is  
395 applied on these same particles perpendicularly to this plane. This observation may be related to the  
396 wood behavior, for which is commonly observed mechanical properties more than 10 times in the  
397 longitudinal direction of the rod.

398

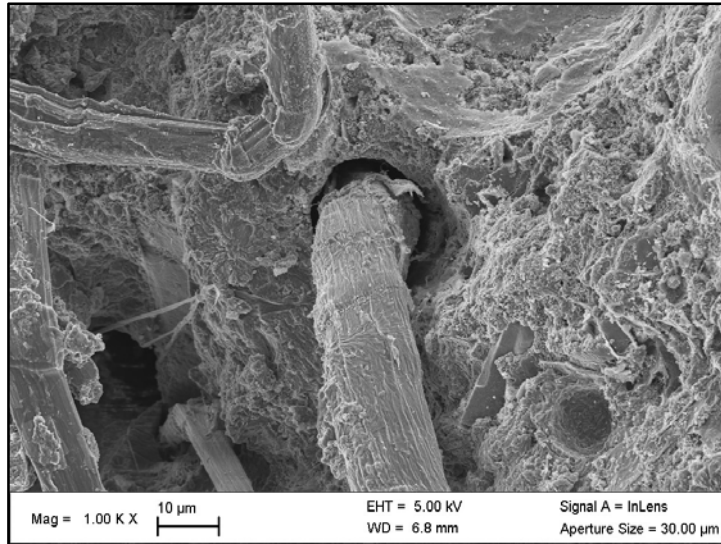


399

400 **Fig. 15.** Mechanical behavior of HC and FHC during a compressive test depending on the direction of  
 401 compaction.

402 In perpendicular orientation, HC has initially a quasi-linear behavior up to the maximum stress of  
 403 about 0.63 MPa. Then, the material continues to be deformed but the stress decreases. For hemp  
 404 concrete with 10% flax fibers (FHC), the same behavior is observed. However, the maximum stress is  
 405 0.79 MPa, 25% higher than HC. In addition, a different mechanical behavior is observed for FHC in  
 406 large strains (above 4% strain). Indeed, the stress remains high while continuing to be deformed.  
 407 Indeed, the stress remains high while continuing to deform. For FHC, the stress is equal to 0.76 MPa at  
 408 12% strain, while it is 0.36 MPa for HC. Thus, flax fibers allow creating reinforcement in the composite  
 409 material. They limit the cracks opening and slow the concrete failure. Fig. 16 shows a SEM image  
 410 showing the typical interface between a flax fiber and a cementitious matrix [21].



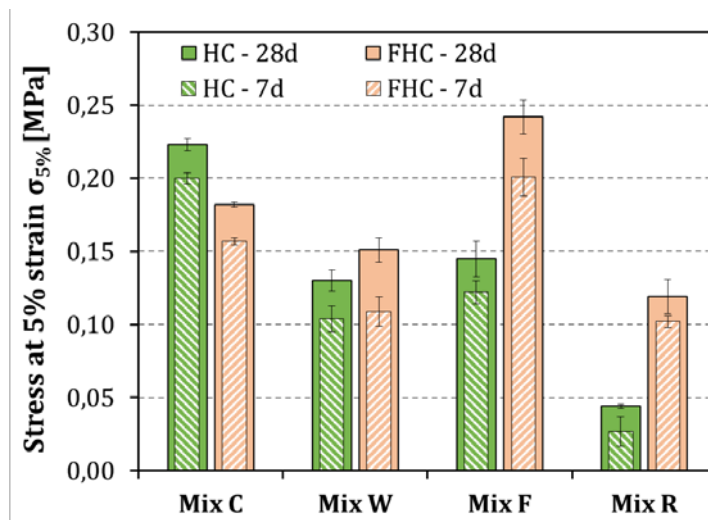


411

412 **Fig. 16.** SEM observation of a typical interface between a flax fiber and a cementitious matrix [21].

413 *3.3.2. Compressive strength at 5 % strain in parallel orientation*

414 The compression test was carried out on all the mixtures for samples stressed in parallel to the  
 415 compacting direction. As it can be seen in Fig. 15, hemp concrete has a quasi-linear behavior for a  
 416 compression in parallel to the compacting direction. There is no maximum stress value; the resistance  
 417 continues to increase until the end of the test, at 12% deformation. To compare the results between  
 418 them, the resistance at 5% strain was defined as the acceptable maximum stress.



419

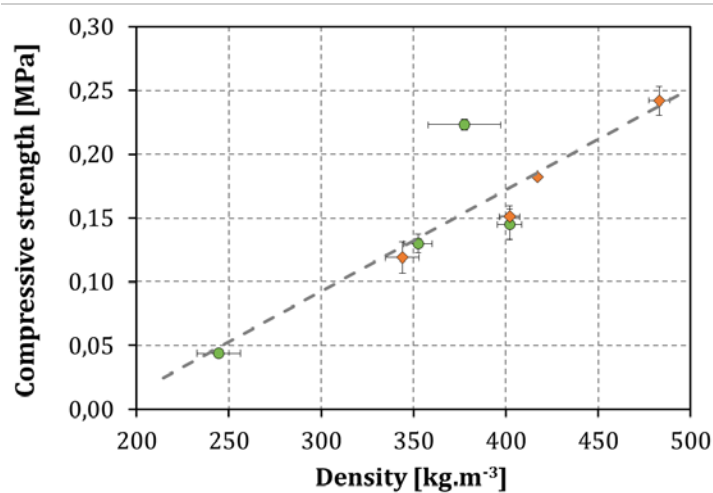
420 **Fig. 17.** Compressive strength at 5% strain for HC and FHC with a loading in parallel to the compaction

421 direction after 7 and 28 days curing.

422 From Fig. 17, it can be seen that the incorporation of flax fibers into the concrete has a positive  
423 effect for mix W, F and R, respectively with an increase in resistance of 16 %, 67 % and 170 % after 28  
424 days curing. Only mix C, which has the lowest amount of hemp, has better resistance with HC; a  
425 decrease in strength of about 18% is observed for the hybrid hemp -flax composite.

426 As it can be seen in Fig. 18, there is a relationship between the effect of flax fibers on hemp concrete  
427 strength and the density. From these results, the resistance improvement of the composites would be  
428 due to the increased density of samples. Indeed, hemp-flax composite density has increased relative to  
429 standard hemp concretes. This increased density is related to an improvement of the compactness of  
430 the material, allowed by the incorporation of fibers into the mixture. Indeed, the fibers having a less  
431 porous structure and a very small diameter, they were able to fit into the intergranular voids of the  
432 hemp concrete.

433 In addition, as shown in Fig. 8, flax fibers absorb less water than hemp shives. Thus, the amount of  
434 water available for the binder is greater, which may limit the hydration and setting problems regularly  
435 observed with hemp concrete.



436

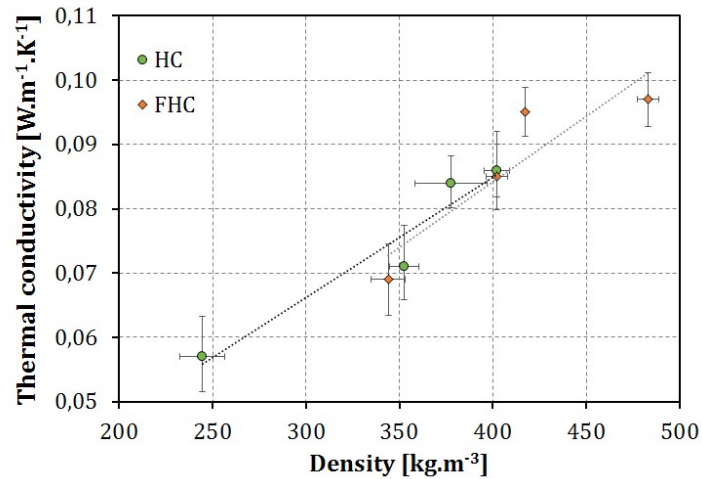
437

**Fig. 18.** Compressive strength (28 days) according to the density.

### 438 3.4. Thermal conductivity

439 The thermal conductivity of HC and FHC composites was measured in dry state (drying at 60°C in  
440 an oven for 48 hours). Fig. 19 presents the variation of thermal conductivity in function of density. The

441 results show a linear relation between thermal conductivity and hempcrete density. This relationship  
442 has already been highlighted by several authors who have been interested in the thermal  
443 characteristics of hemp concrete [8,18,19].



444

445 **Fig. 19.** Thermal conductivity of HC and FHC composites according to their density.

446 It seems that FHC mixes follows the same logic than HC composites for the thermal conductivity.  
447 For HC, the thermal conductivity varied between 0.057 and 0.086 W.m<sup>-1</sup>.K<sup>-1</sup>. However, the thermal  
448 conductivity ranged between 0.069 to 0.097 W.m<sup>-1</sup>.K<sup>-1</sup> for FHC mixes. These higher thermal  
449 conductivity values are related to the higher density of the flax-hemp concrete formulations. However,  
450 all the values obtained for the thermal conductivity coefficient are still very low. Therefore, the FHC  
451 composites can also be considered as a building material with good thermal performances.

#### 452 **4. Conclusion**

453 A new eco-friendly composite material for building construction has been developed by using hemp  
454 shiv and flax fibers as vegetable aggregates and a lime-based binder. To assess the performance of the  
455 composite material, various tests were performed on the composite material and on the conventional  
456 hemp concrete.

457 First, the water absorption test carried out on the plant aggregates showed the very high capacity  
458 for water absorption of hemp shives, almost 450% after 48 hours. Flax fibers had a water absorption  
459 about twice lower than that of hemp shiv (215% after 48 hours). It was also shown that the water

460 absorption of hemp shives and flax fibers follow a logarithmic law. The water absorption of plant  
461 aggregates is known to be problematic for agro-concretes. The lowest water absorption of flax fibers  
462 is thus an advantage to formulate bio-aggregate based concretes.

463 Then flax fibers have improved the mechanical behavior of hemp concrete on two different points.  
464 Firstly, the incorporation of the flax fibers has increased the ductility of the hemp concrete. Even in  
465 large deformations (above 5%), the hybrid hemp-flax concrete retains its almost maximum  
466 compressive strength. Secondly, hybrid concrete has reached better compressive strength (at 5%  
467 strain) for the formulations intended for shuttered wall, floor insulation and roof insulation.

468 Concerning the capillary water absorption, a general trend due to the incorporation of flax fibers  
469 could not be observed. However, the hybrid composite appears to have a lower water absorption than  
470 hemp concrete mixtures containing a lower amount of vegetable particles (external rendering and  
471 floor insulation). A linear relationship between the coefficient of absorption and the capillary  
472 aggregates/paste ratio was observed with hemp concrete. This relation cannot however be observed  
473 for the hybrid hemp-flax composite. This could be explained by an increased complexity of the concrete  
474 porosity, and an increased tortuosity of the capillary networks.

475 The shrinkage of these two materials was also measured. Hemp-flax hybrid concretes showed a  
476 lower shrinkage of about 15% compared to conventional hemp concrete.

477 Finally, values obtained for the thermal conductivity coefficient are still very low. Therefore, hybrid  
478 composite may also be considered as an insulating construction material.

479 Thus, the incorporation of 10% flax fibers in hempcrete composition has allowed to make an  
480 insulating cementitious composite having improved performances compared to conventional hemp  
481 concrete. Further researches are needed to find the optimal replacement of hemp shiv by flax fibers.  
482 Furthermore, additional test is needed to be conducted in order to better quantify the porosity of these  
483 two materials. Finally, the fibers were usually used in concrete to increase their tensile strength. From  
484 the same perspective, it would be interesting to realize bending tests for this material.

485 **Funding**

486 This research did not receive any specific grant from funding agencies in the public, commercial, or  
487 not-for-profit sectors.

488 **References**

- 489 [1] ADEME, Chiffres clés du bâtiment - Édition 2013, ADEME, 2013. <http://www.ademe.fr/chiffres->  
490 [cles-batiment-edition-2013](http://www.ademe.fr/chiffres-cles-batiment-edition-2013) (accessed October 22, 2014).
- 491 [2] M.-P. Boutin, C. Flamin, S. Quinton, G. Gosse, Etude des caractéristiques environnementales du  
492 chanvre par l'analyse de son cycle de vie, INRA - ADEME, 2006.  
493 [http://agriculture.gouv.fr/IMG/pdf/chanvre\\_rapport\\_final\\_d235d.pdf](http://agriculture.gouv.fr/IMG/pdf/chanvre_rapport_final_d235d.pdf).
- 494 [3] P. Bouloc, Le chanvre industriel - Production et utilisations, Éd. France agricole, Paris, 2006.
- 495 [4] S. Amziane, M. Sonebi, Overview on Biobased Building Material made with plant aggregate,  
496 RILEM Tech. Lett. 1 (2016) 31–38. doi:10.21809/rilemtechlett.2016.9.
- 497 [5] A.D. Tran Le, C. Maalouf, T.H. Mai, E. Wurtz, F. Collet, Transient hygrothermal behaviour of a hemp  
498 concrete building envelope, Energy Build. 42 (2010) 1797–1806.  
499 doi:10.1016/j.enbuild.2010.05.016.
- 500 [6] A. Evrard, A. De Herde, Hygrothermal performance of lime-hemp wall assemblies, J. Build. Phys.  
501 34 (2010) 5–25. doi:10.1177/1744259109355730.
- 502 [7] P. Glé, E. Gourdon, L. Arnaud, Acoustical properties of materials made of vegetable particles with  
503 several scales of porosity, Appl. Acoust. 72 (2011) 249–259.  
504 doi:10.1016/j.apacoust.2010.11.003.
- 505 [8] R. Walker, S. Pavía, Moisture transfer and thermal properties of hemp–lime concretes, Constr.  
506 Build. Mater. 64 (2014) 270–276. doi:10.1016/j.conbuildmat.2014.04.081.

- 507 [9] S. Amziane, L. Arnaud, *Bio-aggregate-based building materials - Applications to hemp concretes*,  
508 Wiley-ISTE, London, 2013. <http://onlinelibrary.wiley.com/book/10.1002/9781118576809>  
509 (accessed October 20, 2014).
- 510 [10] L. Arnaud, E. Gourlay, *Experimental study of parameters influencing mechanical properties of*  
511 *hemp concretes*, *Constr. Build. Mater.* 28 (2012) 50–56. doi:10.1016/j.conbuildmat.2011.07.052.
- 512 [11] Y. Diquélou, E. Gourlay, L. Arnaud, B. Kurek, *Impact of hemp shiv on cement setting and*  
513 *hardening: Influence of the extracted components from the aggregates and study of the interfaces*  
514 *with the inorganic matrix*, *Cem. Concr. Compos.* 55 (2015) 112–121.  
515 doi:10.1016/j.cemconcomp.2014.09.004.
- 516 [12] S. Elfordy, F. Lucas, F. Tancret, Y. Scudeller, L. Goudet, *Mechanical and thermal properties of lime*  
517 *and hemp concrete (“hemcrete”) manufactured by a projection process*, *Constr. Build. Mater.*  
518 22 (2008) 2116–2123. doi:10.1016/j.conbuildmat.2007.07.016.
- 519 [13] R. Walker, S. Pavia, R. Mitchell, *Mechanical properties and durability of hemp-lime concretes*,  
520 *Constr. Build. Mater.* 61 (2014) 340–348. doi:10.1016/j.conbuildmat.2014.02.065.
- 521 [14] M. Chabannes, E. Garcia-Diaz, L. Clerc, J.-C. Bénézet, *Studying the hardening and mechanical*  
522 *performances of rice husk and hemp-based building materials cured under natural and*  
523 *accelerated carbonation*, *Constr. Build. Mater.* 94 (2015) 105–115.  
524 doi:10.1016/j.conbuildmat.2015.06.032.
- 525 [15] C. Niyigena, S. Amziane, A. Chateauneuf, L. Arnaud, L. Bessette, F. Collet, G. Escadeillas, C. Lanos,  
526 M. Lawrence, C. Magniont, S. Marceau, S. Pavia, U. Peter, V. Picandet, M. Sonebi, R. Walker, *RRT3:*  
527 *statistical analysis of hemp concrete mechanical properties variability*, in: *Proc. 1st Int. Conf. Bio-*  
528 *Based Build. Mater., RILEM, Clermont-Ferrand, France, 2015: pp. 334–340.*
- 529 [16] V. Nozahic, S. Amziane, G. Torrent, K. Saïdi, H. De Baynast, *Design of green concrete made of plant-*  
530 *derived aggregates and a pumice–lime binder*, *Cem. Concr. Compos.* 34 (2012) 231–241.  
531 doi:10.1016/j.cemconcomp.2011.09.002.

- 532 [17] T.-T. Nguyen, V. Picandet, S. Amziane, C. Baley, Influence of compactness and hemp hurd  
533 characteristics on the mechanical properties of lime and hemp concrete, *Eur. J. Environ. Civ. Eng.*  
534 13 (2009) 1039–1050. doi:10.1080/19648189.2009.9693171.
- 535 [18] T.T. Nguyen, V. Picandet, P. Carre, T. Lecompte, S. Amziane, C. Baley, Effect of compaction on  
536 mechanical and thermal properties of hemp concrete, *Eur. J. Environ. Civ. Eng.* 14 (2010) 545–  
537 560. doi:10.1080/19648189.2010.9693246.
- 538 [19] V. Cérézo, Propriétés mécaniques, thermiques et acoustiques d'un matériau à base de particules  
539 végétales : approche expérimentale et modélisation théorique, PhD thesis, Ecole Nationale des  
540 Travaux Publics de l'Etat, 2005.  
541 <http://www.sudoc.abes.fr/DB=2.1//SRCH?IKT=12&TRM=09460973X&COOKIE=U10178,Klecteurweb,D2.1,E1288a28c-30e,I250,B341720009+,SY,A\9008+1,,J,H2-26,,29,,34,,39,,44,,49-50,,53-78,,80-87,NLECTEUR+PSI,R79.141.14.118,FN> (accessed April 5, 2015).
- 544 [20] K. Charlet, J.-P. Jernot, J. Breard, M. Gomina, Scattering of morphological and mechanical  
545 properties of flax fibres, *Ind. Crops Prod.* 32 (2010) 220–224.  
546 doi:10.1016/j.indcrop.2010.04.015.
- 547 [21] T. Le Hoang, M. Boutouil, F. Khadraoui, M. Gomina, Mechanical and microstructural  
548 characterization of flax fibre-reinforced cement composite, in: *Proc. 11th Jpn.-Korea-Fr.-Can. Jt. Semin. Geoenvironmental Eng., Paralia, Caen, France, 2012: pp. 131–136.*  
549 [http://www.paralia.fr/editions\\_paralia\\_catalogue\\_872.htm](http://www.paralia.fr/editions_paralia_catalogue_872.htm).
- 551 [22] Construire en Chanvre, Règles professionnelles d'exécution d'ouvrages en bétons et mortiers de  
552 chanvre, SEBTP, SEBTP, Paris, France, 2012.  
553 [http://librairie.sebtp.com/product\\_book\\_info/livres-environnement-c-91\\_114/construire-en-chanvre-regles-professionnellesexecution-edition-2012-p-297#.VpKBOE-NqZk](http://librairie.sebtp.com/product_book_info/livres-environnement-c-91_114/construire-en-chanvre-regles-professionnellesexecution-edition-2012-p-297#.VpKBOE-NqZk).
- 555 [23] S. Amziane, F. Collet, Round Robin Test for hemp shiv characterisation: Part 2, bulk density and  
556 particle size distribution, Springer Edition, Edited by S. Amziane, 2016.

- 557 [24] S. Amziane, F. Collet, Round Robin Test for hemp shiv characterisation: Part 3, thermal  
558 conductivity, Springer Edition, Edited by S. Amziane, 2016.
- 559 [25] F. Collet, J. Chamoin, S. Pretot, C. Lanos, Comparison of the hygric behaviour of three hemp  
560 concretes, *Energy Build.* 62 (2013) 294–303. doi:10.1016/j.enbuild.2013.03.010.
- 561 [26] C. Igathinathane, L.O. Pordesimo, E.P. Columbus, W.D. Batchelor, S. Sokhansanj, Sieveless particle  
562 size distribution analysis of particulate materials through computer vision, *Comput. Electron.  
563 Agric.* 66 (2009) 147–158. doi:10.1016/j.compag.2009.01.005.
- 564 [27] EN 933-2, Tests for geometrical properties of aggregates - Determination of particle size  
565 distribution, (1996).
- 566 [28] S. Chafei, F. Khadraoui, M. Boutouil, M. Gomina, Effect of flax fibers treatments on the rheological  
567 and the mechanical behavior of a cement composite, *Constr. Build. Mater.* 79 (2015) 229–235.  
568 doi:10.1016/j.conbuildmat.2014.12.091.
- 569 [29] M. Chabannes, V. Nozahic, S. Amziane, Design and multi-physical properties of a new insulating  
570 concrete using sunflower stem aggregates and eco-friendly binders, *Mater. Struct.* (2014).  
571 doi:10.1617/s11527-014-0276-9.
- 572 [30] V. Nozahic, S. Amziane, Influence of sunflower aggregates surface treatments on physical  
573 properties and adhesion with a mineral binder, *Compos. Part Appl. Sci. Manuf.* 43 (2012) 1837–  
574 1849. doi:10.1016/j.compositesa.2012.07.011.
- 575 [31] S. Amziane, F. Collet, Round Robin Test for hemp shiv characterisation: Part 1, evaluation of initial  
576 water content and water absorption, Springer Edition, Edited by S. Amziane, 2016.
- 577 [32] NF P15-433, Méthodes d'essais des ciments - Détermination du retrait et du gonflement, (1994).
- 578 [33] EN ISO 8894, Refractory materials - Determination of thermal conductivity - Hot-wire method,  
579 (2010).



- 580 [34] A. Franco, An apparatus for the routine measurement of thermal conductivity of materials for  
581 building application based on a transient hot-wire method, *Appl. Therm. Eng.* 27 (2007) 2495–  
582 2504. doi:10.1016/j.applthermaleng.2007.02.008.
- 583 [35] M. Chabannes, J.-C. Bénédet, L. Clerc, E. Garcia-Diaz, Use of raw rice husk as natural aggregate in  
584 a lightweight insulating concrete: An innovative application, *Constr. Build. Mater.* 70 (2014) 428–  
585 438. doi:10.1016/j.conbuildmat.2014.07.025.
- 586 [36] V. Nozahic, *Vers une nouvelle démarche de conception des bétons de végétaux lignocellulosiques*  
587 *basée sur la compréhension et l'amélioration de l'interface liant/végétal - Application à des*  
588 *granulats de chenevotte et de tige de tournesol associés à un liant ponce/chaux*, PhD thesis,  
589 Université Blaise Pascal - Clermont-Ferrand II, 2012. [http://tel.archives-ouvertes.fr/tel-](http://tel.archives-ouvertes.fr/tel-00822142)  
590 [00822142](http://tel.archives-ouvertes.fr/tel-00822142).
- 591 [37] M. Sonebi, S. Wana, S. Amziane, J. Khatib, Investigation of the mechanical performance and  
592 weathering of hemp concrete, in: *Proc. 1st Int. Conf. Bio-Based Build. Mater.*, RILEM, Clermont-  
593 Ferrand, France, 2015: pp. 416–421.
- 594 [38] C. Magniont, *Contribution à la formulation et à la caractérisation d'un écomatériau de*  
595 *construction à base d'agroressources*, PhD thesis, Université Paul Sabatier - Toulouse III, 2011.  
596 <http://thesesups.ups-tlse.fr/980/>.
- 597 [39] F. Murphy, R. Walker, S. Pavia, An assessment of some physical properties of lime-hemp concrete,  
598 in: Ni Nuallain, Walsh, West, Cannon, Caprani, McCabe, University College Cork, Ireland, 2010.  
599 <http://www.tara.tcd.ie/handle/2262/57402> (accessed January 12, 2016).
- 600 [40] A. Kashtanjeva, M. Sonebi, S. Amziane, Investigation of the mechanical performance and drying  
601 shrinkage of hemp concrete, in: *Proc. 1st Int. Conf. Bio-Based Build. Mater.*, RILEM, Clermont-  
602 Ferrand, France, 2015: pp. 309–315.